Journal of Materials Chemistry B

Accepted Manuscript

ROYAL SOCIETY OF CHEMISTRY

www.rsc.org/materialsB

Journal of
Materials Chemistry B

Cite this: DOI: 10.1039/c0xx00000x

www.rsc.org/xxxxxx

Full paper

Dissection of the structure-forming from the structure-guiding activity of silicatein: a biomimetic molecular approach to print optical fibers

Werner E.G. Müller, * Thorben Link, Heinz C. Schröder, Michael Korzhev, Meik Neufurth, David Brandt and Xiaohong Wang *

Received (in XXX, XXX) Xth XXXXXXXXX 20XX, Accepted Xth XXXXXXXXX 20XX
DOI: 10.1039/b000000x

The silicateins, a group of proteins forming the proteinaceous axial filaments of the inorganic biosilica spicules of the siliceous sponges, are unique in their dual function to exhibit both structure-guiding (providing the structural platform for the biosilica product) and structure-forming activity (enzymatic function: biosilica synthesis from ortho-silicate). The primary translation product of the silicatein gene comprises a signal peptide, a pro-peptide and, separated by an autocatalytic cleavage site glutamine/aspartic acid [Q/D], the sequence of the mature silicatein protein. In order to dissect the biocatalytic, structure-forming activity of silicatein from its structure-guiding function two mutated genes were constructed based on the silicatein-α gene of the demosponge *Suberites domuncula*. (i) A gene encoding for a non-processed silicatein that was mutated, by replacing Q/D [Gln (Q)/Asp (D)] by Q/Q, at the cleavage site within the primary translation product between the pro-peptide and the mature enzyme of wild type silicatein. (ii) A gene encoding for a mature enzymatically-active silicatein in which the S-stretch was replaced by a Q-stretch. The enzymatic activity of the mutated protein was significantly enhanced in the presence of the sponge-specific silicatein-interacting protein, silintaphin-1. The two recombinant proteins were applied for micro-contact printing. Using this technique, parallel layers (diameter 10 μm) of the enzymatically inactive, non-processed silicatein were printed onto a gold surface and used as a structure-guiding template for coating with the soluble enzymatically active silicatein. The experiments revealed that after enzymatic reaction with ortho-silicate substrate a biosilica mantle is formed that can act as light waveguide.

1 Introduction

Optical fibers are widely used in fiber-optic-based communication systems since they enable signal transmission with less energy loss than electrical metal wires. In addition, optical-based transmission is less prone to electromagnetic disturbances. Optical fibers are made of extruded glass or organic polymers [1]. There is only one animal/metazoan taxa that is able to fabricate high quality/high purity amorphous silicon dioxide [silica; SiO_2] fibers that have the property to act, like the commercially used fibers in optic communication, as flexible transparent light waveguides, the siliceous sponges with their skeletal elements, the spicules [2-4]. The silica spicules have a length ranging from a few micrometers up to three meters [5] and show a purity of quartz glass [6]. The exceptional feature of those biologically formed structures is that they are synthesized at ambient mild conditions, in contrast to the solely chemically synthesized glass fibers. The decisive difference is that in biochemical reactions enzymes are involved that catalyze the formation of covalent linkages and, by that, accelerate the rates of the chemical reactions by well over a million-fold due to their capacity to lower the activation energy of these reactions. It is still mystery why the sponges keep those light transmitting structures, the spicules, since over 500 million years of evolutionary history [7]. Some experiments suggest that the precise arrangement of those skeletal elements in sponges act as neuronal-like system during information transmission [8,9].

The discovery that the major protein(s) identified in the spicules of the siliceous sponges, the silicateins [10,11], act as true enzymes (reviewed in: [12,13]) contributed to a paradigm shift in the understanding of biomineralization processes. The silicateins are the principle structural and functional proteins that exist in the axial filament of the spicules and comprise a family of three subunits, termed silicatein-α, -β and -γ, with a size between 27 and 29 kDa [10]. Initially, the silicateins have been identified in demosponges, e.g. *Tethya aurantium* [10,11] and *Suberites domuncula* [14] but thereafter they have also been discovered in hexactinellidian sponges, e.g. *Crateromorpha meyeri* [15], or *Aulosaccus* sp. [16]. The primary translation sequence of the silicatein gene from *S. domuncula* comprises a signal peptide, followed by the pro-peptide and the mature enzyme [10,11,14,17].

The signal peptide is removed from the pre-pro-silicatein during its secretion into the intracellular organelles [14,18]. The separation of the mature protein from the pro-peptide proceeds at the autocatalytic cleavage site Gln [Q]/Asp [D]. Besides of the characteristic catalytic triad of the silicateins, distinguishing them from the cathepsins, which consists of Ser [S], instead of Cys [C] in the cathepsins, His [H], and Asn [N], the silicateins comprise a Ser [S] stretch, which has been implicated in the binding to a silica template [19]. During formation of spicules the silicatein molecules associate to fractal-like aggregates [20,21] and form 8 to 10 nm thick nanofibrils [22] that bundle together to ≈ 100 nm thick nanofibril bundles, the subsequent higher hierarchical stage [18]; Fig. 1. The individual nanofibrils start to form biosilica layers. After reaching a size of about 1 µm the individual nanofibrils, arranged in the bundles, form in the consecutive hierarchical stage the axial filaments [23]. During this process, that occurs in the extracellular space, within the mesohyl of the animals, a collagen cast is formed around the spicules (reviewed in: [12]). This net of collagen fibers in the cytoplasm, formed from contractile collagen-secreting sponge cells the amoebocytes [24], is assumed to undergo a process of constriction resulting in "precision biosilica molding". During this process the silica mantel is compressed and elongated (Fig. 1). This shape/morphology formation occurs both at the longitudinal and the lateral planes of the spicules.

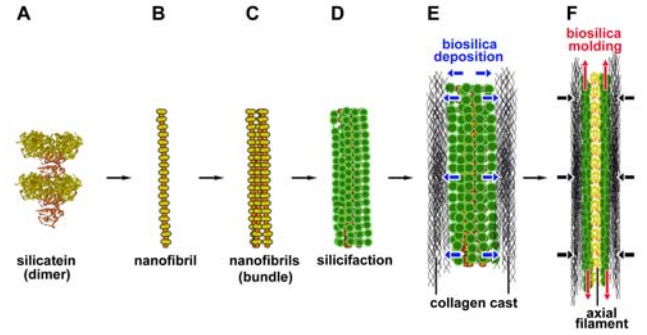

Fig. 1. Formation of biosilica spicules of sponges, based on the structure-forming and structure-guiding function of silicatein; schematic outline. (**A**) The mature silicatein molecules have the property to dimerize and subsequently to oligo- and finally to polymerize to form (**B**) nanofibrils of a diameter of ≈ 8-10 nm. (**C**) Those nanofibrils associate laterally to nanofibrils that compose bundles. (**D**) Due to their structure-forming, enzymatic activity the silicatein nanofibrils, and subsequently the fibril bundles, synthesize biosilica around their surfaces. (**E**) In a subsequent process the growing spicule forms an increasing voluminous biosilica mantel around the central organic core (axial filament), composed of silicatein fibrils. The biosilica deposition proceeds in radial direction (outwards directed arrows). (**F**) Simultaneously, the growing spicule is pressed against a cast formed of collagenous fibers. This constriction results in a compression (inwards directed arrows) and, in turn, a hardening, of the silica mantel. In addition, the fibers elongate (upwards and downward directed arrows), a process termed "biosilica molding" during which the silicatein-built axial filament separates from the silica mantel.

We have unequivocally shown that silicatein is a genuine enzyme catalyzing the polycondensation reaction of ortho-silicate to biosilica (reviewed in: [12,13]) at concentrations around its Michaelis constant of 100 µM, with respect to ortho-silicate [25]. The activity of the silicatein-mediated biosilica formation *in vitro* correlates well with the extent of the biosilica synthesis (spicule formation) in intact animals [26]. The subsequent processes that result in the transformation of the initially formed soft biosilica into the hard rod-like silica spicules involve (*i*) phase separation [27] and (*ii*) a process of syneresis. During the latter step reaction water is extruded that accumulates during the polycondensation reaction [28].

The further distinguishing feature of the enzyme protein is that it comprises, besides of its catalytic, structure-forming function, a structure-guiding property [17]. The latter characteristics is based on the propensity of silicatein to undergo formation of fractal aggregates [20,21]. To study these two functions separately, structure-guiding *versus* structure-forming activity, we constructed in the present study two silicatein genes that were mutated at two functional, characteristic sites. As the starting cDNA we used the silicatein-α gene from *S. domuncula* [14,29]. This approach will provide in the future the option to use a variety of proteins, others than silicatein, as a structure-forming proteinaceous platform onto which silicatein with its enzymatic function can deposit enzymatically a biosilica coat.

First, we constructed a gene (termed *SUBDOSILICa_Q/S*) encoding for a mature enzyme which, however, comprises instead of the S-stretch a Q-stretch; by this modification we exchanged the predicted silica-binding site of silicatein (S-stretch) by a Q-stretch, resulting in an increased capacity of the enzyme to form hydrogen bonds [30] with itself and also with other proteins. This proposed role for the mutated protein SILICAaQ/S_SUBDO was proven by adding a functionally inert protein, bovine serum albumin [BSA], and the sponge-specific protein silintaphin-1 [26] to the silicatein-mediated biosilica enzymatic reaction. Silintaphin-1, as a scaffold protein, is the second most abundant protein in the axial filament and is involved in the guiding of biosilica deposition [26].

Second, to make use of the structure-guiding function of silicatein we mutated the cleavage site within the primary translation product at the border between the pro-peptide and the mature enzyme, Q/D by Q/Q. This gene encoding the non-processed silicatein was named *SUBDOSILICa_NP*. The recombinant protein was produced (SILICAaNP_SUBDO) and used as the structure-guiding platform onto which soluble enzymatically active SILICAaQ/S_SUBDO was layered. The data reported herein show that enzymatically active, structure-forming silicatein, SUBDOSILICa_Q/S, coated around printed non-enzymatically acting structure-guiding silicatein SILICaNP_SUBDO, has the property to synthesize biosilica that can act as light waveguide. We suppose that this finding will contribute to a further rational, meaningful application of the system in the formation of novel materials, e.g. the fabrication of micropatterned structures with inherent photocatalytic and semiconducting properties [31].

2 Results

2.1 The mutated silicatein proteins

Two synthetic DNAs were used to prepare the mutated proteins.

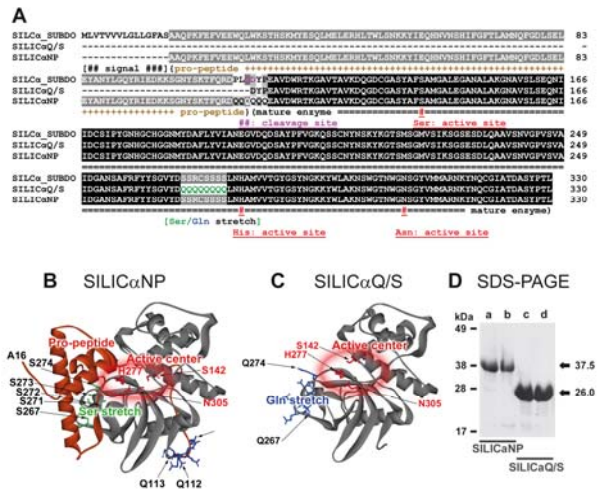

Fig. 2. The mutated silicatein proteins. (**A**) Alignment of the deduced protein from the complete protein sequence of silicatein (SILICα_SUBDO; Krasko et al. 2000) with the mutated mature silicatein (SILICαQ/S) and the mutated non-processed silicatein (SILICαNP). The aa exchange at the cleavage site from Q/D to Q/Q as well as the replacement of the Ser [S]-stretch by the Gln [Q]-stretch are marked. The residues conserved (identical or similar) in all sequences are shown in white on black; those which share similarity to at least two residues are in black on grey. The segments within the wild type non-processed silicatein, the signal peptide [# signal #], the pro-peptide [+++] and the mature enzyme (===) are delimited. The cleavage site within the wild type protein is marked (##); the locations of the catalytically active amino acid moieties within the active site (Ser [S], His [H] and Asn [N]) are marked. The numbering of the aa moieties in the sequences refer to those in the non-processed wild type protein. Model of (**B**) the mutated non-processed silicatein (SILICαNP) and of (**C**) the mutated mature, processed silicatein (SILICαQ/S). The numbers refer to the aa in the non-processed wild type silicatein. The pro-peptide is highlighted in red. The locations of the Ser stretch and the Gln stretch are indicated. The active centers with the catalytically active moieties S, H and N are circled. (**D**) SDS–PAGE analysis of the two recombinantly expressed and purified mutated silicatein proteins. Lanes **a** and **b**, separation of the SILICaNP_SUBDO protein; lanes **c** and **d**, analysis of SILICaQ/S_SUBDO. After electrophoresis the gel was stained by Coomassie Brilliant Blue.

The **NON-PROCESSED SILICATEIN GENE**, comprising the pro-peptide and the mature enzyme encoding stretch, *SUBDOSILICa_NP*, encoded for a silicatein protein in which the border between the pro-peptide and the mature enzyme Q/D was changed to Q/Q within the cleavage site; this position in the protein is located at aa [amino acid]$_{112}$ and aa$_{113}$. The gene was expressed in *Escherichia coli* and termed SILICaNP_SUBDO (Fig. 2A). The purity of the recombinant protein was checked by SDS-PAGE and found to comprise an (almost) pure protein with a size of 37.5 kDa (theoretical M_r of 34,806 and isoelectric point [pI] of 6.9); Fig. 2D lanes a and b. In the wild type silicatein (accession number CAC03737.1) the signal peptide ranges from aa$_1$ to aa$_{15}$. Model prediction of the non-processed silicatein (Fig. 2B) reveals that the pro-peptide stretch (aa$_{16}$ to aa$_{112}$ [with respect to the aa moiety in the non-processed natural silicatein protein; CAC03737.1]) of the silicatein masks the active site of the peptidase (S_{142}, H_{277}, N_{305}). In addition, this pro-peptide covers the S-stretch ranging from S_{267} to S_{274}.

The **MUTATED PROCESSED SILICATEIN** (SILICaQ/S_SUBDO) encodes for a 218 aa long peptide comprising the complete region of the mature protein with its three aa within the active site (S_{142}, H_{277}, N_{305} [numbering on the basis of the complete sequence]); Fig. 2A. The S-stretch is replaced by a Q-stretch ranging from aa$_{267}$ to aa$_{274}$. In this form the active site of the peptide is exposed to the surface of the enzyme (Fig. 2C), as shown by the model. The recombinant protein was expressed in *E. coli* and found to comprise an almost pure protein of a size of 26 kDa (Fig. 2D lanes c and d); the estimated weight is 23,369 and the pI is 8.74.

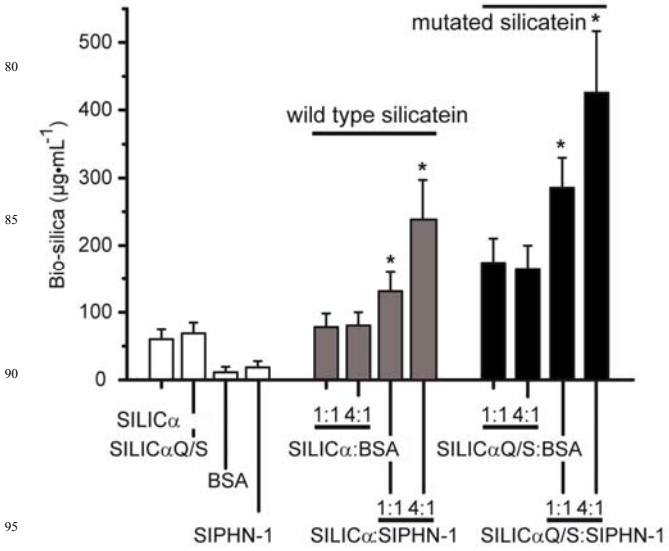

Fig. 3. Stimulating activity of silintaphin-1 on the silicatein-mediated biosilica formation. The enzyme preparations, wild type silicatein-α (SILICα) as well as the mutated silicatein (SILICαQ/S), were incubated either alone or, after co-incubation, with BSA or silintaphin-1 at the stoichiometric ratio 1:1 or 1:4. Prehydrolyzed TEOS was used as a substrate in the standard assay. The results are given as means (10 experiments each) ± standard error of the mean; *$P < 0.01$.

2.2 Biosilica forming activity of the mutated silicatein

The activity of the mutated silicatein-α (SILICaQ/S_SUBDO) was determined in parallel assays with the one of the wild type silicatein-α and using hydrolyzed TEOS as a substrate. During the incubation period chosen (1 h at 22°C) the wild type silicatein-α synthesized 60.3±6.3 µg of biosilica in the 1 mL assay that contained 6 µg enzyme (0.23 mM); the activity of SILICaQ/S_SUBDO is non-significantly higher with 68.9±7.8 µg/6 µg (Fig. 3). The two other proteins tested, BSA (15 µg; 0.23 mM) or silintaphin-1 (10 µg; 0.23 mM), caused almost no

measurable biosilica formation, with 11.7±6.5 µg/6 µg or 17.6±7.9 µg/6 µg, respectively. Co-incubation of silicatein-α with BSA at a 1:1 and 4:1 stoichiometric ratio also did not cause any significant effect on biosilica formation (≈ 80±9 µg/6 µg). In contrast, if BSA is added to SILICaQ/S_SUBDO a significant increase in the biosilica product formation is measured (304.7±42.9 µg/6 µg [1:1 with BSA]; 425.8±89.8 µg/6 µg [4:1 with BSA]); Fig. 3. As expected [26], silintaphin-1 causes a significant increase in silicatein-α-mediated biosilica formation with 131.2±14.1 µg/6 µg [1:1 with silintaphin-1] and with 238.4±28.9 µg/6 µg [4:1].

A strong effect is measured if the mutated silicatein, SILICaQ/S_SUBDO, is added in co-incubation with silintaphin-1 (Fig. 3). In the presence of a 1:1 molar ratio of SILICaQ/S_SUBDO with silintaphin-1 the activity increases from 68.9±7.8 µg/6 µg (absence of silintaphin-1) to 288.3±52.7 µg/6 µg, and even to 439.1±81.9 µg/6 µg (4:1 with respect to silintaphin-1). These data show that the activity of SILICaQ/S_SUBDO is positively affected by both the control protein, BSA, and especially by the specific silicatein-interactor, by silintaphin-2.

In parallel experiments it was established that the mutated non-processed silicatein (SILICaNP_SUBDO) does not cause any measurable activity to form biosilica, if assayed alone or in the presence of BSA or silintaphin-1 (data not shown).

2.3 Wild type silicatein and biosilica deposition

The axial filaments of the isolated siliceous spicules of the sponge *S. domuncula* were freed from the silica mantel by dissolution with hydrofluoric acid. SEM analysis shows that those filaments have dimensions of around 1 µm and are 100-150 µm long. The surface morphology suggests a plaited structure of the highly organized interwoven filament, composed of ≈ 100 nm thick bundles (Fig. 4A; [18]). These bundles have been shown to be composed of approximately 10 nanofibrils measuring 8–10 nm diameter each [22]. The important point to mention is that axial filaments/bundles/nanofibrils are composed of silicatein and hence own the potential to synthesize biosilica [22]. In the initial phase, scales of biosilica are formed on the surface of the axial filaments, after incubation with hydrolyzed TEOS (Fig. 4B).

2.4 µCP of silicatein on the gold surface

Using the biological blueprint for patterning of biosilica onto a silicatein-composed axial filament we applied the µCP technique to layer enzymatically-inert silicatein onto gold plates and coated those structures with enzymatically active silicatein. In turn, we patterned the gold plates with PDMS stamps that were "inked" with enzymatically inactive non-processed SILICaNP_SUBDO, as described under "Material and Methods". After contact printing the samples were inspected microscopically and found to display a regular parallel 10 µm spaced pattern of silicatein (Fig. 4C and D). The silicatein origin of the pattern seen by laser microscopy was proven by applying specific antibodies, directed against silicatein (PoAb-aSilic). After incubation the immunocomplexes were visualized by Cy2-labeled species-specific secondary antibodies (Fig. 4E). In a control reaction, the patterned surfaces were reacted with control, pre-immune serum. Under those conditions no staining could be seen (Fig. 4F).

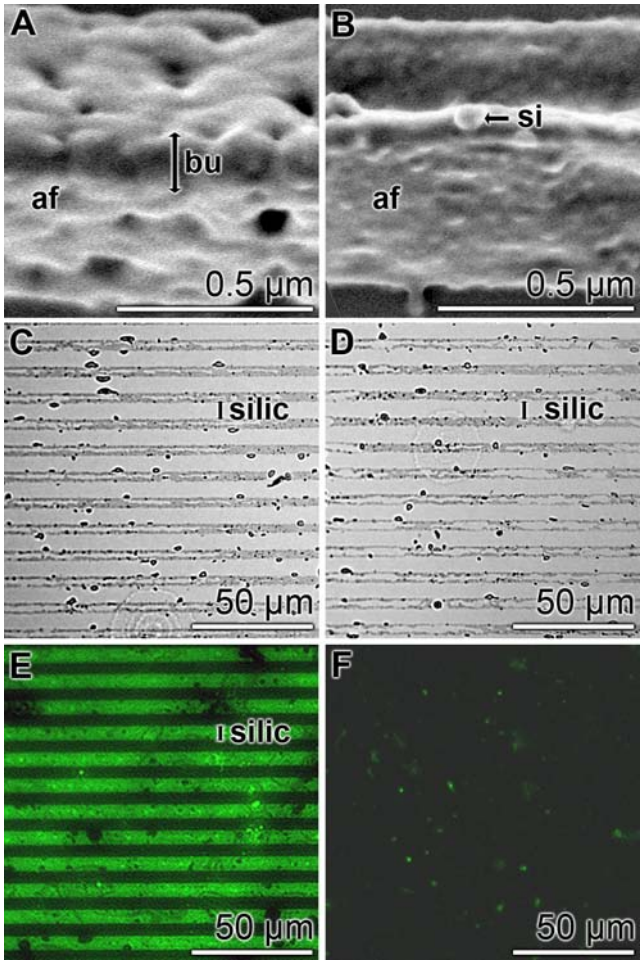

Fig. 4. Bioinspired micro-contact printing (µCP). (**A**) Nature, like sponges, forms within their spicules an organic filament, the axial filament (af), that is compiled of inter-woven bundles (bu). (**B**) After incubation of the axial filament (af) with prehydrolyzed TEOS biosilica deposits are layered as silica scales (si) onto the surface of the filaments. (**C** to **F**) µCP of silicatein onto gold surfaces, using enzymatically inactive non-processed SILICaNP_SUBDO. (**C** and **D**) The regular and parallel silicatein pattern (doubled-headed line: silic) is shown by laser microscopy. (**E**) The specimens were reacted with antibodies raised against silicatein (PoAb-aSilic); then the immunocomplexes were visualized by Cy2-labeled species-specific secondary antibodies. (**F**) In a control reaction the gold pattern surfaces were reacted with a control antiserum.

2.5 µCP of the inactive silicatein-protein pattern followed by layering with the silicatein enzyme

In order to dissect the two properties of silicatein, to act both as structure-guiding protein and as structure-forming protein, the enzymatically inactive, non-processed silicatein, SILICaNP_SUBDO, was printed onto the gold surface. Subsequently those specimens were immersed in a bath containing enzymatically active mutated silicatein, SILICaQ/S_SUBDO. After washing the samples were bathed into a solution, supplemented with hydrolyzed TEOS (ortho-silicate). After incubation a silica mantel is formed around the

SILICaNP_SUBDO/SILICaQ/S_SUBDO printed lines. A scheme is shown in Fig. 5C. Those structures can subsequently act as light waveguide.

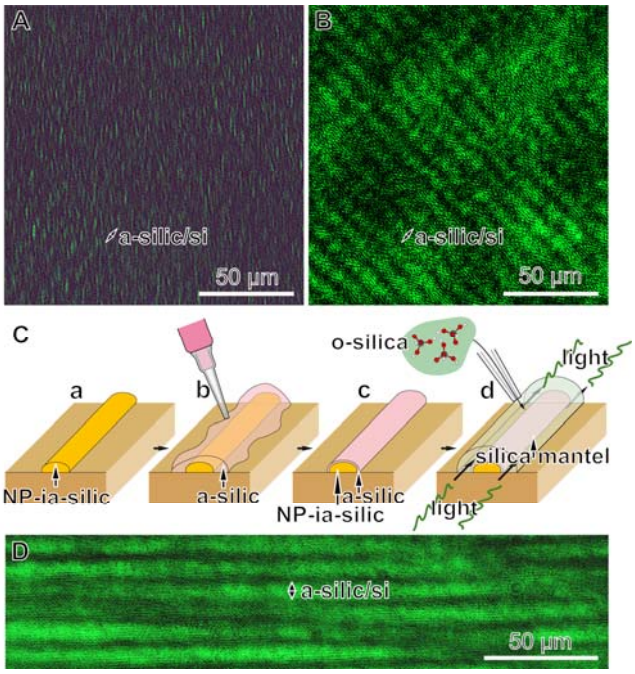

Fig. 5. Bioinspired formation of silica-based waveguides. (**A** and **B**) Light waveguides were formed by enzymatically active silicatein (SILICaQ/S_SUBDO) which was attached to non-enzymatically functioning, structure-guiding silicatein (SILICaNP_SUBDO). Those patterned structures were incubated in hydrolyzed TEOS (ortho-silicate) which is used as substrate for the enzyme to form a silica mantel. One structure/fiber formed from active silicatein and layered onto inactive non-processed silicatein is marked in each image (a-silic/si). As a light source a green laser was used. (A) Control filaments that were not incubated with ortho-silicate; no light transmission is seen along the filaments. (B) Filaments that were incubated with ortho-silicate; after incubation with this enzyme substrate the filaments act as light waveguides after exposure to green laser light. (**C**) Schematic outline of the silica waveguides formed onto enzymatically inactive structure-guiding silicatein (SILICaNP_SUBDO; NP-ia-silic). After bathing those structures and coating them with enzymatically activity silicatein (SILICaQ/S_SUBDO; a-silic), followed by an incubation with ortho-silicate, as the substrate for the enzyme, a biosilica mantel is formed that acts as light waveguide. (**D**) Longer light waveguides exposed to green laser light.

The experiments show that after printing of the non-enzymatically active silicatein (SILICaNP_SUBDO) onto gold surfaces [structure-guiding property of silicatein], followed by subsequent coating of those structures with the soluble active enzyme [structure-forming property of the enzyme] and enzymatic reaction with ortho-silicate, as a substrate, a bright guiding of light through the filaments can be visualized. In the present study the filaments were exposed to green laser light (Fig. 5B and D). However, in a control experiment during which the SILICaNP_SUBDO/SILICaQ/S_SUBDO fibers were not incubated with ortho-silicate no light transmission is seen (Fig. 5A). Using this technique light waveguides with a length of 800 µm had been fabricated; a segment of 400 µm long fibers are shown in Fig. 5D.

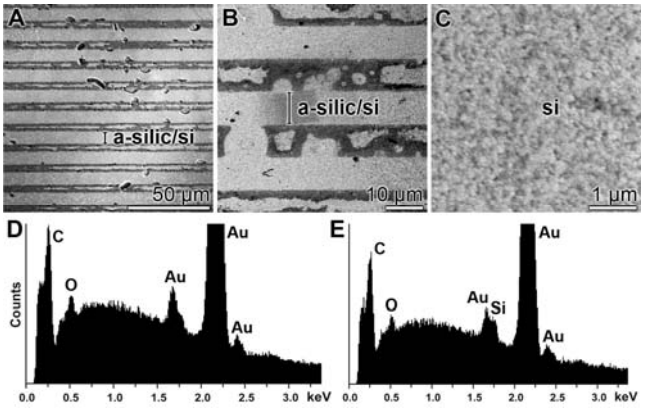

Fig. 6. Element distribution in micro-contact printed filaments that were formed from the structure-guiding SILICaNP_SUBDO, around which active silicatein (structure-forming) was coated (SILICaQ/S_SUBDO). Those filaments were bathed in hydrolyzed TEOS and incubated to allow a silica mantel to be formed (a-silic/si). (**A** and **B**) SEM images of filaments formed from silicatein. In each image one filament is marked (SILICaNP_SUBDO/SILICaQ/S_SUBDO) after incubation with ortho-silicate (a-silic/si). (**C**) High resolution of an area within such a silica-coated filament. The silica nanoparticles (si) are seen. (**D**) EDX analysis of a representative area within a structure-forming/structure-guiding filament which was not incubated with hydrolyzed TEOS. (**E**) EDX analysis within an area of filaments shown in (A) and (B) formed after incubation of the silicatein filaments with hydrolyzed TEOS. The signals for C, O, and Au are shown; the signal/shoulder for Si is prominent in (E).

2.6 Identification of silica on the printed silicatein filaments

The µCP printed enzymatically-inactive silicatein filaments were coated with enzymatically active silicatein. Those structures were exposed to hydrolyzed TEOS. After incubation SEM inspections were performed. At rather low magnifications the parallel 10 µm-thick structures formed from structure-guiding (SILICaNP_SUBDO) and structure-forming (SILICaQ/S_SUBDO) silicatein after incubation with hydrolyzed TEOS are prominent (Fig. 6A and B). At higher magnification the accumulation of the silica nanoparticles, approximately 90 nm in size, is evident (Fig. 6C). In EDX analysis of the areas along the SILICaNP_SUBDO - SILICaQ/S_SUBDO filament, after incubation with hydrolyzed TEOS, the Si element peak becomes prominent (Fig. 6E). This Si-derived peak/shoulder is absent in spectrum of a SILICaNP_SUBDO/SILICaQ/S_SUBDO filament, that was not incubated with hydrolyzed TEOS (Fig. 6D). Since the samples were printed on a gold surface the Au signals are very dominant, besides of those reflecting C and O.

3 Discussion

The aim of 'biologically inspired engineering' is to apply biological principles for the development of new materials and strategies in biomedicine, material sciences, and even sustainable architecture [32]. The siliceous sponge spicules provide an exceptional model for new bioinspired approaches because they make it possible to follow the distinct hierarchical levels, particularly the route(s) from the genes to the molecules, fibrils, fibers, biosilica, and finally, to the morphology [12,13]. Based upon the comprehensive, biology-guided understanding of the synthesis of bioinorganic skeletal elements it becomes now possible to fabricate (bio)materials that might even be superior or more versatile for a given application than the natural model. Focusing on the siliceous spicules, it is well established that these sponge skeletal elements are formed of (almost) pure silica. This chemical high purity is primarily due to the fact that these spicules are synthesized enzymatically, reactions that are known to run substrate-specifically. In addition, the ortho-silicate substrate is taken up from the environment into the cells by transport systems that are likewise substrate-specific [see: 12, 13]. These biomacromolecules, enzymes and transporters, are characterized by affinity constants (K_m values) with values that are close to those of the concentrations existing also in their physiological environment. As an example, the silicic acid transporter, a $Na^+/HCO_3^-[Si(OH)_4]$ co-transporter, which controls the uptake of ortho-silicic acid from the surrounding aqueous milieu is specific for a concentration around 60 µM with respect of ortho-silicic acid [33]. This concentration existed in the early oceans during the period when the sponges evolved [7] and can also be reached in the present-day oceans [34]. The optimal silica concentration for the synthesis of the sponge spicules is between 5 and 100 µM [35]. It can be postulated that the rate of intake of silica in the animals can be accelerated first by binding of silicic acid to less structured proteins, rich in positively charged residues [36], and second by processing of silicic acid to polymeric silica *via* silicatein, which again runs at ≈ 50 µM (see: [12,13]). As known for other enzymes, e.g. alcohol dehydrogenase [37], the strict substrate-specificity is restricted to the respective K_m concentration range. At higher concentrations, like those used for silicatein reactions with titanium(IV) bis-(ammonium lactato)-dihydroxide (Ti[BALDH]) [38] silicatein also accepts structurally related substrates, even though with a reduced affinity.

Future studies must show if a change of the primary and, in consequence, also the secondary and tertiary structure of silicatein by a directed mutation of the gene used for the recombinant preparation will change the affinity of the protein to silica at the expense of an increased affinity to the monomeric substrate. In the present study we focused on the dissection of the characteristic feature of silicatein, first, on the structure-forming (poly-biosilica forming) activity and second, on the structure-guiding function (providing the structural platform for the biosilica product) of silicatein, by mutating the wild type gene. The mature enzymatically-active silicatein, the "structure-forming" enzyme, was mutated at its S-stretch, by replacing the serine residues by glutamine residues. Our assumption that the mutated silicatein comprises an increased propensity to interact with homologous or heterologous molecules via intensified hydrogen bond formation was confirmed experimentally. The mutated silicatein, SILICaQ/S_SUBDO, was found to comprise a significant higher enzymatic activity in the presence of the BSA and the natural silicatein-interacting molecule silintaphin-1. The enhancing effect was very prominent if the silicatein interactor was added at 4:1 molar ratio (silicatein:silintaphin-1) to the mutated enzyme. In a previous study it could be established, and again confirmed now, that the activity of the wild type silicatein is stronger if the enzyme is present in a 4:1 complex with silintaphin-1 [26]. Glutamine is known, as a polar amino acid, to display a high propensity for interacting with its hydrogen bonds to edge strand amino acids [39], especially to those exposed at the β-sheets on surfaces of proteins [40]. In contrast, serine residues in motifs, e.g. the one in the wild type silicatein, promote interhelical hydrogen bond formation [41] and, by that, have been proposed to facilitate interaction with silica (see: [12]). This finding, the replacement of the serine cluster, amino acids with a polar hydroxyl group amino acid, by a glutamine motif, rich in polar amide carbonyl groups, causes in silicatein a change in the functional property of the enzyme.

In the next step of our strategy, outlined in the present study, to apply molecular biomimetics to fabricate materials inspired by nature but designed for a different application we made use of the second property of silicatein, its structure-guiding characteristics. No evidence are available that indicate that the "structure-guiding" property of the mutated protein is changed if compared to the wild-type protein. However, the approach outlined in the present contribution allows a distinct analysis of the "structure-guiding" function, separate from the enzymatic role. Such an approach had not been documented previously [17].

In ealier studies it has been shown that silicatein can form proteinaceous structures based on its fractal abilities [20,21]. In a subsequent study the structure-guiding property of silicatein has been studied in detail and found to be closely associated with the processing/maturation steps of the enzyme [17]. In order to exploit the structure-guiding role of silicatein, separated from its structure-forming function, the cleavage site between the propeptide and the mature enzyme was mutated, allowing a study of the enzymatically inactive non-processed silicatein, SILICaNP_SUBDO. This recombinant protein was micro-contact printed (µCP) onto a gold surface and then coated by the enzymatically active and mutated silicatein, SILICaQ/S_SUBDO. The replicated fiber patterns, formed of non-processed SILICaNP_SUBDO and sheathed by biocatalytically highly active mutated silicatein, SILICaQ/S_SUBDO, forced the formation of a silica mantel that turned out to act as optical fiber.

The successful use of mutated natural molecules/proteins, non-processed silicatein fibers along with a mutated highly active silicatein with an improved tendency to associate with other proteinaceous templates, will substantially contribute to the development and fabrication of new bioinspired materials with a targeted technological application. Obvious future products which should be realized include silica fibers doped with titanium. Silicateins can use, not only ortho-silicate and hydrolyzed TEOS but also titanium [42,31] and organotriethoxysilanes [43] as substrates. It has been demonstrated that the enzyme, under consumption of Ti[BALDH], forms an alkoxide-like conjugate of titanium and finally titanium dioxide that anneals to amorphous/partially

nanocrystalline TiO_2. In addition, organotriethoxysilanes polycondensate to polysilsesquioxanes, polymers that are widely used in personal care but also in optics, electronics and coatings [38]. This unusual wide range of substrate acceptance of the enzyme for those and other metal(loid) oxides, silica, titania and gallium oxohydroxide has been attributed to a certain degree of flexibility of the active center of the molecule [31] (reviewed in: [44]). The fields of application of those new (bio)materials, e.g. titanium doped silica/glass fibers, are wide. Optical silica fibers, doped with silica, comprise not only an improved refractive index but also allow the fabrication of highly radiation sensitive step-index multimode and single mode fibers (see: [45]), and even allow the production of efficient affinity probes for phosphopeptide enrichment [46], characterized by favorable thermal expansion coefficients [47].

The advantages of the µCP technology, using wild type or mutated silicateins are evident; the process can be performed at physiological, ambient conditions and in turn can be applied also on organic surfaces. While µCP is usually performed at ultra-flat surfaces of metals, silicon or glass substrates, others, even organic, surfaces can be chosen as well. This diversity is due to the fact that in addition to a functionalization of the surfaces by chemical or physical/gaseous processes, the printed material, here silicatein, can be modified to meet the given conditions. Applying again molecular biological approaches, specific tags can be applied to increase the affinity of silicatein, e.g., to gold by adding a Cys-tag to the molecule [31], or by using a Glu-tagged silicatein which displays high affinity to hydroxyapatite [48]. The long-term goal of our studies in this field will be the construction of a silica-based optical computer composed of optical fibers with the characteristics of non-linear refractive indices and of having a small bandgap energy and, by that, allowing a two-photon absorption [49]. The use of the enzymatically-active silicatein protein, devoid of any structure-guiding activity, will open in the future a technology to coat defined organic or inorganic fibers, e.g. also carbon nanotubes, with a biosilica mantel acting as an insulator. *Vice versa* the structure-forming property of silicatein will allow the synthesis of highly flexible fibers which are decorated with non-silica materials, like self-assembled calcite nanocrystals [50]. Finally, silicatein-formed organic fibers can be used as a core to deposit self-assembled calcitic nanocrystals, constituting extremely flexible light waveguides [50]. These examples highlight some opportunities of the application of the two mutated proteins, the non-processed silicatein as structure-guiding template and the Q-stretch-containing mature silicatein as a structure-building enzyme, in the manufacturing of flexible nanowires for the application of electronic and/or optical devices and circuits [51].

4 Material and Methods

4.1 Materials

The sources for the enzymes and reagents, used for the molecular biological experiments, were listed previously [52]. Bovine serum albumin (# A4612), tetraethyl orthosilicate (TEOS; # 759414) and gold foil (#326518) were purchased from Sigma (Taufkirchen; Germany).

4.2 Recombinant silicatein and silintaphin-1 preparations

The recombinant proteins of silicatein and silintaphin-1 were prepared as follows:

WILD TYPE SILICATEIN-α: This recombinant protein (SILICa_SUBDO), the short, mature silicatein-α, was prepared as previously described [14]. In brief, the silicatein-α cDNA (accession number CAC03737.1) from *S. domuncula* was inserted into the oligohistidine expression vector pQE30 (Qiagen, Hilden; Germany) and used for transformation of *Escherichia coli* BL21 (Novagen/Merck, Darmstadt; Germany). After induction of the bacteria with isopropyl thio-β-D-galactoside, the recombinant protein was purified by affinity chromatography, unfolded in urea/imidazole, and finally refolded in the 50 mM Tris/HCl buffer (0.5 M L-arginine, glutathione [9 mM glutathione / 1 mM oxidized glutathione] redox couple, 0.3 M NaCl, 1 mM KCl). The final protein concentration was 110-130 µg • mL^{-1}.

MUTATED SILICATEINS: The two mutated genes, first the one encoding the non-processed silicatein (*SUBDOSILICa_NP*) and second the mature silicatein in which the nucleotides encoding for the S-stretch were replaced by those encoding for a Q-stretch (*SUBDOSILICa_Q/S*), have been synthetically prepared by GeneArt® (Life Technologies, Darmstadt; Germany). The complete genes were assembled from synthesized oligonucleotides using the GeneAssembler® process. The constructs had been cloned into a standard cloning vector. From those genes the recombinant proteins were prepared as follows. Both synthetic genes, *SUBDOSILICa_NP* (EMBL accession number HG964668) and *SUBDOSILICa_Q/S* (EMBL accession number HG964669), were optimized to achieve maximum levels of productivity in the *E. coli* host. The fragments were cloned into the pENTR221 vector using attB1 and attB2 cloning sites. The plasmid DNA was purified from transformed bacteria; the final sequences of the constructs were verified by sequencing.

The Gateway System from Invitrogen (Darmstadt; Germany) was used for efficient LR recombination reaction with attR containing pDEST17 destination vector (Invitrogen). After transformation in TOP10 *E. coli* cells, the clones were analyzed by checking polymerase chain reaction [PCR] followed by sequencing. Positive expression clones were transformed into competent BL21-AI One Shot cells (Invitrogen) were specifically designed for recombinant protein expression from T7-based expression vectors. The cells were grown in LB-medium at 37°C under vigorous shaking until the OD_{600} reaches 0.6-0.8. After adding the inductor, 0.2% L-arabinose, the cells were further incubated overnight. The cells were pelleted by centrifugation. The recombinant proteins, SILICaNP_SUBDO (from the *SUBDOSILICa_NP* gene) and SILICaQ/S_SUBDO (*SUBDOSILICa_Q/S*), were isolated by application of the PROFINIA system (Bio-Rad, Munich; Germany) as described [53]. In brief, clear lysate (volume of 30 ml) was purified on one-mL Bio-Scale Mini Profinity IMAC Cartridges, using the following buffer steps: (*i*) 6 M urea (50 mM KH_2PO_4, pH 8.0; 5 mM mM imidazole, 300 mM KCl), (*ii*) 6 M urea (50 mM KH_2PO_4, pH 8.0; 10 mM imidazole, 300 mM KCl) and (*iii*) 6 M urea (50 mM KH_2PO_4, pH 8.0; 250 mM imidazole, 300 mM KCl).

The recombinant proteins were analyzed by sodium dodecyl sulfate polyacrylamide gel electrophoresis (SDS-PAGE) as follows. Samples of 5 µg of protein were mixed with loading

buffer (Roti-Load; Carl Roth, Karlsruhe; Germany), boiled and subjected to SDS-PAGE (15% acrylamide and 0.1% SDS) as described [54]. The gels were stained with Coomassie brilliant blue.

SILINTAPHIN-1: The complete silintaphin-1 cDNA (accession number CAP16640.1) was cloned into the expression vector pTrcHis2-TOPO (Invitrogen, Karlsruhe; Germany) and then transferred into *E. coli* BL21 cells [55]. The recombinant protein (SIPHN-1_SUBDO) was purified by affinity chromatography and stored in the above mentioned 50 mM Tris/HCl buffer at a concentration of ≈ 80 µg • mL^{-1}.

4.3 Modeling of the silicateins

The crystal structure of the mutated human cathepsin S (2.2 Å resolution) has been published [56]. Based on this template a structure prediction of the SILICaNP_SUBDO and SILICaQ/S_SUBDO was performed as described previously [17] and using the Modeller Program package [57] (www.Salilab.org).

4.4 Determination of silicatein enzymatic activity

The details of the determination of the enzymatic activity of silicatein were given before [14,26]. In those standard assays, samples of 1 mL were prepared in 50 mM Tris/HCl buffer (pH 7.4; 150 mM NaCl) containing 6 µg of purified recombinant silicatein-α or mutated silicatein SILICaQ/S_SUBDO. Following the description given earlier, the enzyme samples were mixed with either bovine serum albumin (BSA; 66 kDa) or recombinant silintaphin-1 [55]; 43 kDa) at a stoichiometric ratio of 1:1 and 4:1. After pre-incubation for 10 min (30 min, 22°C) the silicatein/silintaphin-1-BSA assays were subjected to enzyme activity determination. As substrate 200 µM prehydrolyzed TEOS (tetraethyl orthosilicate) was chosen, as the last component. Acid hydrolysis [58] was performed as previously described, with a 1:5 molar ratio of TEOS/H_2O in 10 mM HCl for 10 min. The enzymatic reactions were run at 22°C for 1 h under shaking. Then, the samples were centrifuged (10,000 ***g***, 30 min, 4°C) and, after washing with ethanol, the sedimented silica was treated with 2 M NaOH for 30 min (30°C) to hydrolyze biosilica formed. The concentration of the liberated, soluble silicic acid was determined by the molybdenum blue colorimetric method [10], applying the Silicon Test colorimetric assay kit (Merck #1.14794, Darmstadt; Germany). A calibration curve of a silicon standard (Merck #1.09947) was used to calculate the absolute amounts of silicic acid from the obtained absorbance values at 795 nm.

4.5 Isolation of the axial filament from spicules of S. domuncula

For our biologically inspired engineering of micro-scale patterning of silicatein on gold surface we took advantage from the appearance, form, shape and dimension of the axial filament which resides in the siliceous spicules of *S. domuncula* [18]. In turn those organic filaments were isolated from the spicules (tylostyles) obtained from sponge tissue; the axial filament was isolated from them by dissolution of the silica material with hydrofluoric acid (2 M HF/8 M NH_4F; pH 5) at room temperature overnight [10].

4.6 Electron microscopy

Scanning electron microscopy (SEM) analysis of the axial filament was performed with a Zeiss DSM 962 Digital Scanning Microscope (Zeiss, Aalen; Germany). The samples were mounted onto aluminum stubs (SEM-Stubs G031Z; Plano, Wetzlar; Germany) that were covered with adhesive carbon (carbon adhesive Leit-Tabs G3347). Prior to analysis, the samples were sputtered with a 20-nm-thin layer of gold in argon plasma (Bal Tec Med 020 coating system; Bal Tec, Balzers; Liechtenstein).

4.7 Micro-contact printing (µCP) of silicatein on the gold surface

Lines were printed onto gold plates using the micro-contact printing (µCP) approach, as described [31,59,60]. Polydimethoxysilane (PDMS) stamps, comprising a pattern of arrays of lines (width: 10 µm; length: 500 µm) and spaced by about 10 µm were used. The PDMS stamps were fabricated by soft-lithography (AMO, Aachen; Germany). The stamp was cleaned with 2-propanol and, then, loaded with the recombinant mutated SILICaNP_SUBDO (5 µg in 250 mL TBS [Tris-buffered saline]) by dipping. The stamp was placed for 20 s isogonally with the plate of gold foil (Au{111}; thickness 0.25 mm) at room temperature (RT). Then the sample was extensively washed with TBS; after a short air drying step (2 min) the specimen was stored in a humid chamber until further use.

In continuation, the samples were analyzed by a VK-8710K Color 3D Laser Microscope (Keyence, Stuttgart; Germany) or by immunodetection. Immunodetection of the printed silicatein, immobilized onto the Au surfaces, was performed with polyclonal antibodies directed against native silicatein-α [18]. The rabbit antibodies (PoAb-aSilic) were reacted in a 1:1,000 dilution (in 15% blocking solution [Roche Applied Science, Mannheim; Germany]) with the silicatein (SILICaNP_SUBDO) that was printed onto the gold surface, during an incubation period of 90 min (RT). In a series of controls the silicatein patterns onto the gold surfaces were incubated with control, pre-immune serum. After blocking, the immunocomplexes were visualized with Cy2-labeled species-specific secondary antibodies (90 min, RT) (Dianova, Hamburg; Germany). For visualization, the samples were inspected by immunofluorescence microscopy (Olympus AHBT3 light microscope/AH3-RFC reflected light fluorescence), using the 488 nm filter.

4.8 Fabrication of biosilica fibers onto a µCP silicatein pattern

Where indicated, the silicatein-printed Au surfaces, layered with SILICaNP_SUBDO, were incubated with a solution of 20 µg/mL mature, mutated silicatein (SILICaQ/S_SUBDO) solution in 50 mM Tris/HCl buffer (pH 7.4; 150 mM NaCl) für 5 h at RT. To obtain biosilica micropatterns, the silicatein-printed Au surfaces were incubated in an aqueous solution of 200 µM prehydrolyzed TEOS (14 h, RT). Subsequently, the specimens were extensively washed to remove the nonreacted ortho-silicate precursor and the biosilica micropatterns were inspected by scanning electron microscopy (SEM) and energy-dispersive X-ray spectroscopy (EDX).

The SEM/EDX analyses were performed as described recently [61].

4.9 SEM and energy-dispersive X-ray analysis

The procedure used has been described [62]. In brief, SEM analysis was performed with a HITACHI SU 8000 (Hitachi High-Technologies Europe GmbH, Krefeld; Germany) that was employed at low voltage (<1 keV; analysis of near-surface organic surfaces). The beam deceleration mode was applied to improve the scanning records [63]. For energy-dispersive X-ray (EDX) spectroscopic analysis the SEM microscope was coupled to an XFlash 5010 detector [64].

4.10 Exposure of the biosilica fibers to laser light

The biosilica fibers fabricated after µCP onto silicatein pattern, were inspected under an Olympus AHBT3 light microscope with an attached CCD-Camera (Colorview12; Olympus, Münster; Germany). The fibers were coupled in the dark with a free-spaced green laser source (Hyperion Multi-Color Laser Source; XiO Photonics, Enschede; The Netherlands) at 532 nm with a power of 5-6 mW; the diameter of the laser light fiber was 200 µm. The images were documented at a 40x magnification.

4.11 Additional methods

For the quantification of protein, the described Bradford method [65] was used with the indicator Roti-Quant (Roth). The results were statistically evaluated [66].

5 Conclusions

In conclusion, the results of the present study provide a conceptual and practical framework for a next generation of molecular biomimetics by fabrication of biomaterials, built upon changes of the "wild type" organic platforms by mutations in the genetic blueprint, based on the results of causal analytical studies.

Acknowledgements

W.E.G. M. is a holder of an ERC Advanced Investigator Grant (No. 268476 BIOSILICA). This work was supported by grants from the Deutsche Forschungsgemeinschaft (Schr 277/10-3), the European Commission (CoreShell: No. 286059; Bio-Scaffolds: No. 604036; MarBioTec*EU-CN*: No. 268476; and BlueGenics: No. 311848) and the International Human Frontier Science Program.

Notes and references

ERC Advanced Investigator Grant Research Group, Institute for Physiological Chemistry, University Medical Center of the Johannes Gutenberg University Mainz, Duesbergweg 6, D-55128 Mainz, Germany. Tel.: +49 6131-39-25910; Fax: +49 6131-39-25243; E-mail: wmueller@uni-mainz.de (Prof. W.E.G. Müller) and wang013@uni-mainz.de (Prof. X.H. Wang).

1 M. Mignanelli, K. Wani, J. Ballato, S. Foulger and P. Brown, *Opt. Express*, 2007, **15**, 6183-6189.
2 R. Cattaneo-Vietti, G. Bavestrello, C. Cerrano, A. Sarà, U. Benatti, M. Giovine and E. Gaino, *Nature*, 1996, **383**, 397-398.
3 V. C. Sundar, A. D. Yablon, J. L. Grazul, M. Ilan and J. Aizenberg, *Nature*, 2003, **424**, 899-900.
4 W. E. G. Müller, K. Wendt, C. Geppert, M. Wiens, A. Reiber and H. C. Schröder, *Biosensors and Bioelectronics*, 2006, **21**, 1149-1155.
5 X. H. Wang, H. C. Schröder and W. E. G. Müller, *Int. Rev. Cell Mol. Biol.*, 2009, **273**, 69-115.
6 W. E. G. Müller, K. Jochum, B. Stoll and X. H. Wang, *Chem. Mater.*, 2008, **20**, 4703-4711.
7 X. H. Wang, S. Hu, L. Gan, M. Wiens and W. E. G. Müller, *Terra Nova*, 2010, **22**, 1-11.
8 W. E. G. Müller, X. H. Wang, H. C. Schröder, M. Korzhev, V. A. Grebenjuk, J. S. Markl, K. P. Jochum, D. Pisignano and M. Wiens, *FEBS J.*, 2010, **277**, 1182-1201.
9 A. S. Rivera, N. Ozturk, B. Fahey, D. C. Plachetzki, B. M. Degnan, A. Sancar and T. H. Oakley, *J. Exp. Biol.*, 2012, **215**,1278-1286.
10 K. Shimizu, J. Cha, G. D. Stucky and D. E. Morse, *Proc. Natl. Acad. Sci. USA*, 1998, **95**, 6234-6238.
11 J. N. Cha, K. Shimizu, Y. Zhou, S. C. Christiansen, B. F. Chmelka, G. D. Stucky and D. E. Morse, *Proc. Natl. Acad. Sci. USA*, 1999, **96**, 361-365.
12 X. H. Wang, H. C. Schröder, K. Wang, J. A. Kaandorp and W. E. G. Müller, *Soft Matter*, 2012, **8**, 9501-9518.
13 W. E. G. Müller, H. C. Schröder, Z. Burghard, D. Pisignano and X. H. Wang, *Chemistry - A European Journal*, 2013, **19**, 5790-5804.
14 A. Krasko, B. Lorenz, R. Batel, H. C. Schröder, I. M. Müller and W. E. G. Müller, *Europ. J. Biochem.*, 2000, **267**, 4878-4887.
15 W. E. G. Müller, X. H. Wang, K. Kropf, A. Boreiko, U. Schloßmacher, D. Brandt, H. C. Schröder and M. Wiens, *Cell Tissue Res.*, 2008, **333**, 339-351.
16 G. N. Veremeichik, Y. N. Shkryl, V. P. Bulgakov, S. V. Shedko, V. B. Kozhemyako, S. N. Kovalchuk, V. B. Krasokhin, Y. N. Zhuravlev and Y. N. Kulchin, *Mar. Biotechnol.*, 2011, **13**, 810-819.
17 H. C. Schröder, X. H. Wang, Manfrin A, Yu SH, Grebenjuk VA, Korzhev M, M. Wiens, Schloßmacher U and W. E. G. Müller, *J. Biol. Chem.*, 2012, **287**, 22196-22205.
18 W. E. G. Müller, M. Rothenberger, A. Boreiko, W. Tremel, A. Reiber and H. C. Schröder, *Cell Tissue Res.*, 2005, **321**, 285-297.
19 C. C. Perry and Y. Lu, *Faraday Transactions*, 1992, **88**, 2915-2921.
20 M. M. Murr and D. E. Morse, *Proc. Natl. Acad. Sci. USA*, 2005, **102**,11657-11662.
21 W. E. G. Müller, A. Boreiko, U. Schloßmacher, X. H. Wang, M. N. Tahir, W. Tremel, D. Brandt, J. A. Kaandorp and H. C. Schröder, *Biomaterials*, 2007, **28**, 4501-4511.
22 W. E. G. Müller, E. Mugnaioli, H. C. Schröder, U. Schloßmacher, M. Giovine, U. Kolb and X. H. Wang, *Cell Tissue Res.*, 2013, **351**, 49-58.
23 G. Croce, A. Frache, M. Milanesio, L. Marchese, M. Causà, D. Viterbo, A. Barbaglia, V. Bolis, G. Bavestrello, C. Cerrano, U. Benatti, M. Pozzolini, M. Giovine and H. Amenitsch, *Biophys. J.*, 2004, **86**, 526-534.
24 A. V. Ereskovsky, The Comparative Embryology of Sponges, Springer, Heidelberg, 2010.
25 W. E. G. Müller, U. Schloßmacher, X. H. Wang, A. Boreiko, D. Brandt, S. E. Wolf, W. Tremel and H. C. Schröder, *FEBS J.*, 2008, **275**, 362-370.
26 U. Schloßmacher, M. Wiens, H. C. Schröder, X. H. Wang, K. P. Jochum and W. E. G. Müller, *FEBS J.*, 2011, **278**, 1145-1155.
27 X. H. Wang, U. Schloßmacher, H. C. Schröder and W. E. G. Müller, *Soft Matter*, 2013, **9**, 654-664.
28 X. H. Wang, H. C. Schröder, D. Brandt, M. Wiens, I. Lieberwirth, G. Glasser, U. Schloßmacher, S. F. Wang and W. E. G. Müller, *ChemBioChem*, 2011, **12**, 2316-2324.
29 W. E. G. Müller, A. Boreiko, X. H. Wang, S. I. Belikov, M. Wiens, V. A. Grebenjuk, U. Schloßmacher and H. C. Schröder, *Gene*, 2007, **395**, 62-71.
30 N. Eswar and C. Ramakrishnan, *Protein Eng.*, 2000, **13**, 227-238.
31 M. Wiens, T. Link, T. A. Elkhooly, S. Isbert and W. E. G. Müller, *Chem. Comm.*, 2012, **48**,11331-11333.
32 W. E. G. Müller, X. H. Wang, K. P. Jochum and H. C. Schröder, *IUBMB Life*, 2013, **65**, 382-396.
33 H. C. Schröder, S. Perović-Ottstadt, M. Rothenberger, M. Wiens, H. Schwertner, R. Batel, M. Korzhev, I. M. Müller and W. E. G. Müller, *Biochem. J.*, 2004, **381**, 665-673.
34 M. Maldonado, M. C. Carmona, M. J. Uriz and A. Cruzado, *Nature (London)*, 1999, **401**, 785-788.
35 M. E. Jewell, *Ecol. Monogr.*, 1935, **5**, 461-504.

36 T. Ikeda and A. Kuroda, *Colloids Surf. B Biointerfaces*, 2011, **86**, 359-363.

37 D. W. Crabb, M. Matsumoto, D. Chang and M. You, *Proc. Nutr. Soc.*, 2004, **63**, 49-63.

38 R. L. Brutchey, J. E. Goldberger, T. S. Koffas and T. D. Tilley, *Chem. Mater.*, 2003, **15**, 1040-1046.

39 C. L. Worth and T. L. Blundell, *BMC Evol. Biol.*, 2010, **10**, 161.

40 J. A. Siepen, S. E. Radford and D. R. Westhead, *Protein Sci.*, 2003, **12**, 2348-2359.

41 J. P. Dawson, J. S. Weinger and D. M. Engelman, *J. Mol. Biol.*, 2002, **316**,799-805.

42 J. L. Sumerel, W. Yang, D. Kisailus, J. C. Weaver, J. H. Choi and D. E. Morse, *Chem. Mater.*, 2003, **15**, 4804-4809.

43 Y. Zhou, K. Shimizu, J. N. Cha, G. D. Stucky and D. E. Morse, *Angew Chemie Intern. Ed.*, 1999, **38**, 779-782.

44 R. L. Brutchey and D. E. Morse, *Chem. Rev.*, 2008, **108**, 4915-4934.

45 M. C. Paul, R. Sen, S. K. Bhadra and K. Dasgupta, *Optical Materials*, 2008, **30**, 1538-1548.

46 F. Wang, Z. Shi, F. Hu, Z. Xia and L. Wang, Tuning of Ti-doped mesoporous silica for highly efficient enrichment of phosphopeptides in human placenta mitochondria. *Anal. Bioanal. Chem.*, 2013, **405**, 1683-1693.

47 V. Pukh, L. Baikova, M. Kireenko and L. Tikhonova, *Advanced Materials Res.*, 2008, **39-40**, 153-158.

48 F. Natalio, T. Link, W. E. G. Müller, H. C. Schröder, F. Z. Cui, X. H. Wang and M. Wiens, *Acta Biomaterialia*, 2010, **6**, 3720-3728.

49 D. Goswami, *Resonance*, 2003, **8**, 56-71.

50 F. Natalio, T. P. Corrales, M. Panthöfer, D. Schollmeyer, W. E. G. Müller, M. Kappl, H. J. Butt and W. Tremel, *Science*, 2013, **339**, 1298-1302.

51 X. H. Wang, H. C. Schröder, W. E. G. Müller, *Trends Biotechnol.*, 2014, in press (doi.org/10.1016/j.tibtech.2014.05.004).

52 W. E. G. Müller, X. H. Wang, V. A. Grebenjuk, M. Korzhev, M. Wiens, U. Schloßmacher and H. C. Schröder, *PLoS ONE*, 2012, **7(4)**, e34617. doi:10.1371/journal.pone.0034617.

53 S. Petersen and L. Usinger, Automated desalting of proteins with the Profina protein purification system: Comparison to manual desalting by dialysis, Bio-Rad Bulletin 5539, 2007.

54 U. K. Laemmli, *Nature*, 1970, **227**, 680-685.

55 M. Wiens, M. Bausen, F. Natalio, T. Link, U. Schlossmacher and W. E. G. Müller, *Biomaterials*, 2009, **30**, 1648-1656.

56 J. P. Turkenburg, M. B. Lamers, A. M. Brzozowski, L. M. Wright, R. E. Hubbard, S. L. Sturt and D. H. Williams, *Acta Crystallogr. D Biol. Crystallogr.*, 2002, **58**, 451-455.

57 A. Sali and T. L. Blundell, *J. Mol. Biol.*, 1993, **234**, 779-815.

58 X. Tong, T. Tang, Z. Feng and B. Huang, *J. Appl. Polym. Sci.*, 2002, **86**, 3532-3536.

59 A. Kumar and G. M. Whitesides, *Appl. Phys. Lett.*, 1993, **63**, 2002-2004.

60 M. R. Monroe, Y. P. Li, S. B. Ajinkya, L. B. Gower and E. P. Douglas, *Materials Sci. Engin.*, 2009, **C29**, 2365-2369.

61 W. E. G. Müller, H. C. Schröder, U. Schlossmacher, V. A. Grebenjuk, H. Ushijima and X. H. Wang, *Biomaterials*, 2013, **34**, 8671-8680.

62 M. Wiens, X. H. Wang, U. Schloßmacher, I. Lieberwirth, G. Glasser, H. Ushijima, H. C. Schröder and W. E. G. Müller, *Calcif. Tissue Intern.*, 2010, **87**, 513-524.

63 A. Endo, M. Yamada, S. Kataoka, T. Sano, Y. Inagi and A. Miyaki, *Colloids Surf. A Physicochem. Eng. Asp.*, 2010, **357**, 11-16.

64 T. Salge and R. Terborg, *Anadolu. Univ. J. Sci. Technol.*, 2009, **10**, 45-55.

65 S. Compton and C. G. Jones, *Anal. Biochem.*, 1985, **151**, 369-374.

66 L. Sachs, Angewandte Statistik, Springer, Berlin, 1984, p. 242.

Colour graphic:

The enzymatically inactive silicatein was used as the platform for the enzymatically active silicatein, which synthesized the silica waveguide.